

---

# WATS: Calibrating Graph Neural Networks with Wavelet-Aware Temperature Scaling

---

**Xiaoyang Li**

Independent Researcher  
Lxy289692485@gmail.com

**Linwei Tao**

School of Computer Science  
University of Sydney  
linwei.tao@sydney.edu.au

**Haohui Lu**

University of Sydney  
haohui.lu@sydney.edu.au

**Minjing Dong**

City University of Hong Kong  
minjdong@cityu.edu.hk

**Junbin Gao**

University of Sydney  
junbin.gao@sydney.edu.au

**Chang Xu**

School of Computer Science  
University of Sydney  
c.xu@sydney.edu.au

## Abstract

Graph Neural Networks (GNNs) have demonstrated strong predictive performance on relational data; however, their confidence estimates often misalign with actual predictive correctness, posing significant limitations for deployment in safety-critical settings. While existing graph-aware calibration methods seek to mitigate this limitation, they primarily depend on coarse one-hop statistics, such as neighbor-predicted confidence, or latent node embeddings, thereby neglecting the fine-grained structural heterogeneity inherent in graph topology. In this work, we propose Wavelet-Aware Temperature Scaling (WATS), a post-hoc calibration framework that assigns node-specific temperatures based on tunable heat-kernel graph wavelet features. Specifically, WATS harnesses the scalability and topology sensitivity of graph wavelets to refine confidence estimates, all without necessitating model retraining or access to neighboring logits or predictions. Extensive evaluations across seven benchmark datasets with varying graph structures and two GNN backbones demonstrate that WATS achieves the lowest Expected Calibration Error (ECE) among all compared methods, outperforming both classical and graph-specific baselines by up to 42.3% in ECE and reducing calibration variance by 17.24% on average compared with graph-specific methods. Moreover, WATS remains computationally efficient, scaling well across graphs of diverse sizes and densities. Code will be released based on publication.

## 1 Introduction

GNNs offer a principled approach for learning over structured data and have achieved strong empirical performance across a wide range of domains, including social network modeling [8], traffic forecasting [28], and healthcare applications [10, 20]. They support key tasks such as node classification [51, 33], link prediction [49, 21], and graph-level inference [50, 12]. While GNNs are widely adopted for their representational power, their output confidence often fails to reflect true predictive reliability, which is an issue of growing concern in high-stakes domains, for instance, medical diagnosis and financial risk assessment.

Model calibration, which measures the alignment between a model’s predicted confidence and its true correctness likelihood [13], is a key aspect of model reliability. A well-calibrated model is expected to produce predictions whose confidence scores accurately reflect the observed accuracy. For example, a prediction made with 70% confidence should be correct 70% of the time. Recent findings highlight that GNNs behave differently from standard independent and identically distributed (*i.i.d.*) trained models such as CNNs and transformers [24, 36, 42]. Unlike CNNs and transformers, which often suffer from overconfidence, GNNs tend to be systematically underconfident: their predicted confidence scores are consistently lower than their true accuracy [40, 16, 19].

Several recent approaches aim to address this issue through graph-aware calibration strategies, including Graph Attention Temperature Scaling (GATS) [16], CaGCN [41], Graph Ensemble Temperature Scaling (GETS) [53], and SimCalib [35]. These approaches typically enhance node-level calibration by integrating neighbour structural cues with their predictive status, such as confidence level.

However, they predominantly rely on shallow neighborhood statistics or opaque latent representations, which may result in unstable and inaccurate uncertainty estimation. As they capture only limited, local information and fail to reflect the broader structural context, leading to unreliable calibration, especially for low-degree scenarios. For illustration, we provide empirical evidence that nodes with similar local statistics can exhibit different miscalibration levels across graphs. Based on the above limitation, we aim to build a method that: (i) flexibly incorporates neighborhood information without relying on additional explicit pretraining status (ii) maintains high calibration performance across diverse graph domains, while remaining lightweight and post-hoc. (iii) performs temperature scaling at the node level to allow identical correction based on multi-hop structural information.

Therefore, in this work, we propose a calibration framework called WAVELET-AWARE TEMPERATURE SCALING (WATS), which introduces flexibly scaled structural features through graph wavelets. We incorporate graph wavelets because they offer a principled way to capture structural information at multiple scales [7]. Our methods, wavelets spatial localization controlled by the scale parameters  $s$  and  $k$ , enabling fine-grained capture of multi-hop dependencies. Differs from graph wavelet algorithms used in neural network [7, 1] in that it does not aim to reconstruct or smooth node features for node classification. Instead, it uses wavelet coefficients as structural signatures to indicate the node uncertainty, which allows WATS to adaptively calibrate predictions based on the underlying structure, helping to correct confidence errors where standard methods fall short. Our main contributions are summarized as follows:

**WATS:** We propose a novel post-hoc calibration framework that performs node-wise temperature scaling using flexibly scaled graph wavelet features.

**Robust, interpretable structural features:** We show that graph wavelet features are stable and geometry-aware, encoding local graph structure without relying on potentially noisy signals such as neighboring logits or distances to labeled nodes.

**Extensive empirical validation:** Across multiple graph benchmarks and GNN architectures. WATS consistently improves calibration quality, reducing ECE and outperforming both classical and graph-specific calibration baselines.

## 2 Related Work

### 2.1 Uncertainty Calibration for Neural Networks

Uncertainty calibration aims to align a model’s predicted confidence with the true likelihood of correctness. Existing approaches are typically divided into two categories: in-training and post-hoc

**In-training** approaches incorporate uncertainty estimation within the model optimization process. For example, Bayesian Neural Networks (BNNs) and variational inference methods achieve this by imposing probabilistic distribution over model parameters [9, 22, 32]. Alternative frequentist strategies, such as conformal prediction [37] and quantile regression [26], are also employed to generate calibrated probability estimates.

**Post-hoc** methods, in contrast, calibrate a pre-trained model without modifying its internal parameters. These include non-parametric techniques such as histogram binning [46] and isotonic regression [47], as well as parametric approaches that assume a specific transformation form, including temperature scaling (TS) [13] and Beta Calibration [18]), to adjust the model’s output logits accordingly.

## 2.2 Graph-Specific Calibration Methods

While post-hoc calibration methods perform well on Euclidean data with CNNs, their effectiveness declines on graph-structured data due to the lack of relational modeling [16, 41]. To address this, several graph-aware approaches have been proposed. CaGCN [41] uses a GCN-based temperature predictor to incorporate structure, while GATS [16] applies attention over neighborhoods for node-specific temperatures. GETS [53] introduces a sparse mixture-of-experts using degree, features, and confidence. SimCalib [35] adds similarity-preserving regularization, and Shi et al. [30] use reinforcement learning to adapt calibration to graph structure. Beyond post-hoc methods, Yang et al. [44] reweight edges during training to improve calibration, and Yang et al. [45] propose a calibration-aware loss targeting underconfidence caused by shallow GNNs. These methods collectively integrate graph structure and node-level signals to enhance calibration.

## 2.3 Graph Wavelet

Graph wavelets provide compact, spatially localized bases that are well suited to graph signal processing and structural representation learning. Whereas classical wavelets such as Haar and Daubechies are defined on Euclidean lattices [3, 25], graph wavelets extend these ideas to non-Euclidean domains by leveraging the spectral properties of the graph Laplacian [5, 31, 43].

A particularly versatile construction is the lifting scheme [34], which can be transferred to graphs without any data-driven training. Hammond et al. [15] further improved practicality by replacing the costly Laplacian eigendecomposition with Chebyshev polynomial approximations, enabling efficient wavelet transforms on large graphs. Since then, graph wavelets have supported a variety of downstream tasks, including graph convolutional architectures [43, 6], multimodal wavelet networks [1], community detection via scale-adaptive filtering [38], and diffusion-based node embeddings that capture multi-scale structural patterns [7]. All these methods and application indicates the importance of Graph wavelet in both theoretical and empirically practice

# 3 Method

## 3.1 Preliminary Study

We address the problem of uncertainty calibration in semi-supervised node classification tasks over graphs. Let  $\mathcal{G} = (\mathcal{V}, \mathcal{E})$  denote a graph, where  $\mathcal{V}$  is the set of nodes and  $\mathcal{E}$  is the set of edges. The adjacency matrix is denoted by  $A \in \mathbb{R}^{N \times N}$ , where  $N = |\mathcal{V}|$ . Each node  $v_i \in \mathcal{V}$  has a feature  $x_i \in \mathcal{X}$ , and for a subset of labeled nodes  $\mathcal{L} \subseteq \mathcal{V}$ , the true label  $y_i \in \{1, \dots, K\}$  is provided. Let  $X = [x_1, \dots, x_N]^\top$  be the feature matrix and  $Y = [y_1, \dots, y_N]^\top$  the label vector, a GNN  $f_\theta$  performs node classification via predicting node-wise class probabilities  $\hat{p}_i(y)$  as

$$\hat{y}_i = \arg \max_y \hat{p}_i(y), \quad \hat{c}_i = \max_y \hat{p}_i(y),$$

where  $\hat{y}_i$  denotes the predicted label and  $\hat{c}_i$  denotes its confidence. In the field of model calibration, a well-calibrated model provides confidence that aligns with the true accuracy well as

$$\mathbb{P}(y_i = \hat{y}_i \mid \hat{c}_i = c) = c \quad \forall c \in [0, 1].$$

The measurement of model calibration can be computed via Expected Calibration Error (ECE) [13] as  $\mathbb{E}[|\mathbb{P}(y_i = \hat{y}_i \mid \hat{c}_i) - c|]$ , however, ECE cannot be easily computed due to limited samples. Thus, an estimation of ECE is introduced by grouping samples into  $M$  bins with equal confidence intervals as  $B_m = \{j \in \mathcal{N} \mid \frac{m-1}{M} < \hat{c}_j \leq \frac{m}{M}\}$ , where  $\mathcal{N}$  is the subset of node that used in evaluation  $\mathcal{N} \subseteq \mathcal{V}$ . Given the bin accuracy  $\text{Acc}(B_m) = \frac{1}{|B_m|} \sum_{i \in B_m} \mathbf{1}(\hat{y}_i = y_i)$  and bin confidence  $\text{Conf}(B_m) = \frac{1}{|B_m|} \sum_{i \in B_m} \hat{c}_i$ , the approximation can be achieved by computing the expected difference between bin accuracy and confidence as

$$\text{ECE} = \sum_{m=1}^M \frac{|B_m|}{|\mathcal{N}|} |\text{Acc}(B_m) - \text{Conf}(B_m)|. \quad (1)$$

### 3.2 Uncertainty Estimation in GNNs

**Calibrate via One-hop Statistics** Message-passing is widely adopted in GNNs, including GCN [17] and GAT [39], which can be simplified via a degree-normalized mean aggregator as

$$h_i^{(\ell+1)} = \frac{1}{d_i + 1} \left( h_i^{(\ell)} + \sum_{j \in \mathcal{N}(i)} h_j^{(\ell)} \right), \quad d_i = |\mathcal{N}(i)|. \quad (2)$$

where  $d_i$  excludes the node itself, so  $d_i + 1$  accounts for the self-loop. The final embedding  $h_i^{(L)}$  induces the confidence  $\hat{c}_i$ . This local aggregation implicitly determines the final prediction and the associated confidence  $\hat{c}_i$  of node  $i$ . Although GATs confines all structural operations, including neighbor temperature aggregation, attention weights, neighbor confidence averaging to 1-hop, and CaGCN and GETS stack two GCN layers to nominally reach 2-hop, each layer itself still performs only 1-hop aggregation. As a result, these methods are unable to adaptively capture longer-range dependencies. Although these calibration techniques show effectiveness, we argue that one-hop statistics only cannot provide an accurate estimation of node uncertainty in GNNs. Considering a simplified one-hop estimator of confidence:

$$\hat{c}_i \approx \frac{1}{d_i + 1} \sum_{j \in \{i\} \cup \mathcal{N}(i)} y_j,$$

where  $y_j \in \{0, 1\}$  is the true label indicator for node  $j$ . Then the per-node calibration bias is

$$\text{bias}_i = |\hat{c}_i - \mathbf{1}(\hat{y}_i = y_i)| \approx \left| y_i - \frac{1}{d_i + 1} \sum_{j \in \mathcal{N}(i)} y_j \right|. \quad (3)$$

As shown in Eq. 3, for example, when  $d_i = 2$  and the neighbor labels are  $[0, 1]$ , the average is  $1/3$  regardless of the true label  $y_i$ , making the estimate uninformative, which means high uncertainty. In sparse or low-homophily regions, one-hop neighborhoods may carry weak or misleading signals, resulting in poor bias approximation. This motivates the need for structure-aware calibration methods that incorporate richer, multi-hop graph information. This expression highlights the critical influence of node degree on predictive uncertainty. Nodes with low degree have limited access to neighborhood information, which in GNNs systematically manifests as underconfidence. That compile with the previous study [16, 41] and illustrated in Figure 1. Conversely, as degree increases, the richer information integration drives the model toward higher confidence estimates.

Moreover, as shown in Figure 1, we observe that even within the same degree range, the ECE varies significantly across graphs. While the overall trend that higher-degree nodes tend to have higher confidence is consistent, the magnitude and pattern of this trend differ per graph. This discrepancy highlights that node degree alone is insufficient to explain calibration behaviors in GNNs.

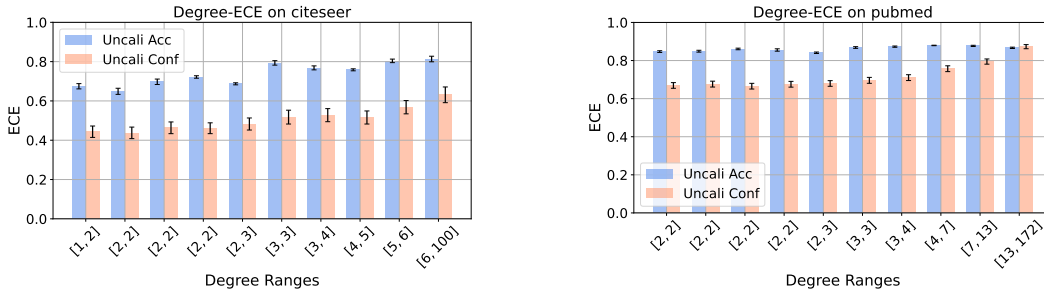


Figure 1: The x-axis shows node degree ranges and the y-axis represents the ECE. The blue bars indicate the uncalibrated accuracy and the pink bars indicate the uncalibrated confidence. Compared to Pubmed, Citeseer exhibits a more noticeable gap between accuracy and confidence in low-degree ranges, highlighting stronger underconfidence in sparse regions.

**Calibrate via Local Structure** While node degree is highly correlated with predictive confidence, this relationship is not consistent across graphs. Our analysis reveals that nodes with similar degree

ranges can exhibit markedly different levels of miscalibration across datasets, indicating that degree is informative but insufficient to fully explain confidence behavior in GNNs. Additionally, the confidence level can also be unstable, making it an unreliable indicator of confidence.

These observations point to a deeper insight: node confidence is influenced not only by immediate neighbors and structures, but also by the broader structural context in which a node is situated. This is further supported by Wang et al. [40], who demonstrate that although deeper GNNs may suffer from reduced accuracy, they tend to exhibit higher confidence, highlighting the importance of extended neighborhood influence. Prior works [40, 16, 35] have emphasized some graph features, such as homophily and node similarity. GETS [53] partially addresses this by incorporating degree embeddings into a mixture-of-experts framework. While all these methods lack the ability to capture multi-hop structural patterns or incorporate unstable confidence. Therefore, addressing the above limitation and improving the calibration requires leveraging multi-hop context and structure-aware features, enabling the model to better handle both under- and over-confidence in structurally diverse regions of the graph.

### 3.3 Wavelet-Aware Temperature Scaling

We propose WATS, a lightweight and effective node-wise calibration framework that can be seamlessly applied to any pretrained GNN with scalability to large graphs. Unlike conventional or graph-specific post-hoc methods that rely on global or one-hop features, WATS introduces a structural perspective by leveraging graph wavelet features with tunable scales.

These wavelet representations capture rich, scalable structural signals [15, 4], often neglected in calibration. By learning a temperature for each node based on its structural embedding, WATS aligns confidence with correctness in a fine-grained, node-specific manner. In addition to its strong empirical performance, WATS is also architecture-agnostic, making it broadly applicable across diverse graph types and calibration scenarios.

#### 3.3.1 Graph Wavelet Transform

Traditional graph signal processing often relies on graph Fourier transform, which projects signals into the spectral domain using the eigenvectors of the normalized graph Laplacian  $\mathbf{L}_{\text{sym}} = \mathbf{I} - \mathbf{D}^{-1/2} \mathbf{A} \mathbf{D}^{-1/2}$  as orthonormal bases. Given a signal  $\mathbf{x} \in \mathbb{R}^N$ , its Fourier transform is defined as  $\hat{\mathbf{x}} = \mathbf{U}^\top \mathbf{x}$  and the inverse as  $\mathbf{x} = \mathbf{U} \hat{\mathbf{x}}$ , where  $\mathbf{U}$  contains the eigenvectors of  $\mathbf{L}_{\text{sym}}$  [31]. While this formulation enables spectral filtering via  $\mathbf{U} g_\theta \mathbf{U}^\top \mathbf{x}$ , it suffers from several limitations [15, 43, 52]: (1) The eigendecomposition of  $\mathbf{L}_{\text{sym}}$  has high computational cost ( $\mathcal{O}(N^3)$ ); (2)  $\mathbf{U}$  is generally dense, making the transform costly for large graphs; (3) The resulting filters lack localization in the vertex domain, limiting their ability to capture localized structural patterns.

To overcome these issues, we adopt the graph wavelet transform, which retains the spectral benefits of Fourier analysis while introducing localization and sparsity. Graph wavelet bases are constructed using a heat kernel scaling function  $g(s\lambda) = e^{-s\lambda}$ , where  $s > 0$  is a scale parameter controlling the diffusion extent. The wavelet operator is defined as:

$$\Psi_s = \mathbf{U} \text{diag}(g(s\lambda_1), \dots, g(s\lambda_N)) \mathbf{U}^\top \quad (4)$$

where  $\lambda_i$  are the eigenvalues of  $\mathbf{L}_{\text{sym}}$ . The inverse transform uses  $g(-s\lambda)$ , yielding efficient localized filtering analogous to diffusion. Direct computation of  $\Psi_s$  is still impractical for large graphs. To address this, we adopt the Chebyshev polynomial approximation to avoid explicit eigendecomposition, following [15, 43]. We first rescale  $\mathbf{L}_{\text{sym}}$  as:  $\hat{\mathbf{L}} = \frac{2}{\lambda_{\max}} \mathbf{L}_{\text{sym}} - \mathbf{I}$ ,  $\lambda_{\max} \approx 2$  and define Chebyshev polynomials  $\{\mathbf{T}_k\}_{k=0}^K$  via the recurrence:  $\mathbf{T}_0 = \mathbf{X}_0$ ,  $\mathbf{T}_1 = \hat{\mathbf{L}} \mathbf{X}_0$ ,  $\mathbf{T}_k = 2\hat{\mathbf{L}} \mathbf{T}_{k-1} - \mathbf{T}_{k-2}$ , for  $k \geq 2$  where  $\mathbf{X}_0$  is the initial input signal. In our setting, we choose  $\mathbf{X}_0$  as the log-degree to preserve structural properties while mitigating skewed degree distributions. Degree encodes a node’s connectivity and its potential for information aggregation in message-passing GNNs, and in previous section, it is proven to be an essential factor of uncertainty. The final wavelet-transformed feature matrix is constructed as:

$$\mathbf{S} = \sum_{k=0}^K \alpha_k \mathbf{T}_k, \quad \text{with } \alpha_k = e^{-sk} \quad (5)$$

Here we are using  $K$ -order Chebyshev polynomial to approximate the wavelet scaling function  $g(s\lambda) = e^{-s\lambda}$ , that is

$$g(s\lambda) \approx \frac{1}{2}c_0 + \sum_{k=1}^K c_k T_k(\lambda)$$

with

$$c_k = \frac{2}{\pi} \int_{-1}^1 \frac{T_k(y)g(sy)}{\sqrt{1-y^2}} dy$$

refer to Hammond et al. [15]  $c_k$  are computable constants before training. Followed by row-wise  $\ell_1$  normalization:

$$\mathbf{H}_i = \frac{\mathbf{S}_i}{\|\mathbf{S}_i\|_1}, \quad \forall i \in \{1, \dots, N\} \quad (6)$$

The hyper-parameter  $k$  sets the maximum receptive-field size (i.e., the number of hops considered), while the scale parameter  $s$  governs the extent of diffusion. A small  $s$  restricts diffusion and thus accentuates local structure, whereas a large  $s$  allows more extensive diffusion, leading to stronger smoothing and the integration of broader, long-range context. In practice, selecting appropriate values for  $k$  and  $s$  enables control over the locality and granularity of the wavelet features. This flexibility is crucial for capturing diverse structural patterns across graphs of varying density and topology.

### 3.3.2 Node-wise Temperature Scaling

Based on the extracted wavelet features, we predict a node-specific temperature parameter to rescale the logits produced by the original GNN. Given the feature matrix  $\mathbf{H} \in \mathbb{R}^{N \times (K+1)}$ , we employ a two-layer multilayer perceptron (MLP) to capture the non-linear relationship and predict the temperatures:

$$\tau_i = \text{Softplus}(\text{MLP}(\mathbf{h}_i)) \quad (7)$$

where  $\mathbf{h}_i$  is the wavelet feature vector for node  $i$ , and Softplus ensures the positivity of the predicted temperatures. This design provides a flexible and efficient mechanism for uncertainty calibration across the graph. The calibrated logits are obtained via post-hoc temperature scaling:

$$\tilde{z}_i = \frac{z_i}{\tau_i}$$

where  $z_i$  is the original output logit from the GNN, and  $\tilde{z}_i$  is the rescaled logit after calibration. The temperature predictor is trained by minimizing the cross-entropy loss on the validation set using the rescaled logits.

## 4 Experiment

### 4.1 Experiment Setting

We evaluate the calibration performance of our proposed WATS method on seven widely-used graph datasets: Cora [23], Citeseer [11], Pubmed [27], Cora-Full [2], Computers [29], Photo [29], and Reddit [14]. These datasets cover a range of graph sizes, feature dimensions, and label complexities, providing a comprehensive benchmark for calibration analysis, detailed graph summary is shown on Appendix.

Following previous practice [41, 16, 35], we adopt two commonly used GNN architectures as base models, which are GCN [17] and GAT [39]. The models are trained under a semi-supervised node classification setting. After training, we perform post-hoc calibration using different methods without modifying the model parameters.

**Training Settings.** Follow the experiment settings [16, 35, 53], We randomly use 20% of nodes for training, 10% for validation and calibration training, and 70% for testing. The detail of training setting is given in the Appendix.

**Calibration Settings.** For each method, calibration parameters are learned on the validation set and evaluated on the test set. Calibration performance is measured using the ECE with 10 bins. The detailed calibration setting are displayed in detail in Appendix.

**Calibration Methods Compared.** We compare several post-hoc calibration methods. TS applies a global temperature to all logits [13], while ETS averages predictions from multiple temperature-tuned models [48]. CaGCN uses a lightweight GCN to learn node-specific temperatures [41], and GATS employs attention-based aggregation over one-hop neighbors [16]. GETS introduces a sparse mixture-of-experts that combines degree, features, and logits [53]. WATS, our proposed method, predicts temperatures using tunable graph wavelet features and rescale logits.

Table 1: Each result is reported as the mean  $\pm$  standard deviation over 10 runs. ‘Uncalib’ refers to uncalibrated outputs, and ‘oom’ indicates out-of-memory failures where the method could not complete. Best performance on ECE are highlighted for each configuration.

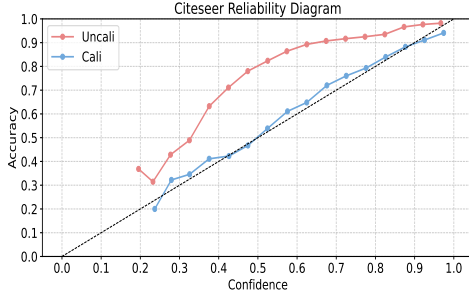
Dataset	Model	Uncalib	TS	ETS	CAGCN	GATS	GETS	WATS
Citeseer	GCN	23.20 $\pm$ 3.21	2.57 $\pm$ 0.78	3.45 $\pm$ 1.03	4.44 $\pm$ 1.47	2.38 $\pm$ 0.65	4.09 $\pm$ 1.36	<b>2.15 <math>\pm</math> 0.48</b>
	GAT	15.61 $\pm$ 1.14	3.22 $\pm$ 0.29	3.55 $\pm$ 0.41	2.77 $\pm$ 0.59	3.22 $\pm$ 0.24	3.80 $\pm$ 2.05	<b>2.67 <math>\pm</math> 0.38</b>
Computers	GCN	5.94 $\pm$ 0.52	3.88 $\pm$ 0.70	3.91 $\pm$ 0.49	2.04 $\pm$ 0.34	3.34 $\pm$ 0.61	2.94 $\pm$ 1.26	<b>1.31 <math>\pm</math> 0.29</b>
	GAT	5.86 $\pm$ 1.26	2.12 $\pm$ 0.19	2.11 $\pm$ 0.20	2.99 $\pm$ 0.64	2.01 $\pm$ 0.17	3.95 $\pm$ 3.73	<b>1.83 <math>\pm</math> 0.28</b>
Cora	GCN	22.44 $\pm$ 1.17	2.25 $\pm$ 0.33	2.20 $\pm$ 0.44	2.79 $\pm$ 0.50	2.98 $\pm$ 0.59	2.96 $\pm$ 0.47	<b>2.13 <math>\pm</math> 0.51</b>
	GAT	17.26 $\pm$ 0.38	2.03 $\pm$ 0.31	<b>1.92 <math>\pm</math> 0.31</b>	2.56 $\pm$ 0.38	2.15 $\pm$ 0.30	2.97 $\pm$ 0.47	2.02 $\pm$ 0.30
Cora-full	GCN	27.79 $\pm$ 0.22	5.06 $\pm$ 0.10	5.00 $\pm$ 0.09	3.87 $\pm$ 0.22	5.13 $\pm$ 0.10	3.11 $\pm$ 1.95	<b>2.04 <math>\pm</math> 0.13</b>
	GAT	37.21 $\pm$ 0.37	2.50 $\pm$ 0.23	1.32 $\pm$ 0.16	4.79 $\pm$ 0.34	2.70 $\pm$ 0.26	2.16 $\pm$ 1.11	<b>1.30 <math>\pm</math> 0.23</b>
Photo	GCN	3.33 $\pm$ 0.22	2.45 $\pm$ 0.22	2.47 $\pm$ 0.20	1.72 $\pm$ 0.22	2.22 $\pm$ 0.19	3.25 $\pm$ 1.63	<b>1.03 <math>\pm</math> 0.18</b>
	GAT	3.21 $\pm$ 0.47	1.81 $\pm$ 0.43	2.34 $\pm$ 0.50	1.71 $\pm$ 0.10	1.80 $\pm$ 0.43	3.05 $\pm$ 1.67	<b>1.63 <math>\pm</math> 0.18</b>
Pubmed	GCN	14.33 $\pm$ 1.20	2.55 $\pm$ 0.38	2.81 $\pm$ 0.47	1.82 $\pm$ 0.36	2.30 $\pm$ 0.52	2.34 $\pm$ 0.51	<b>1.04 <math>\pm</math> 0.07</b>
	GAT	10.67 $\pm$ 0.30	0.88 $\pm$ 0.09	<b>0.87 <math>\pm</math> 0.09</b>	0.91 $\pm$ 0.11	0.89 $\pm$ 0.08	0.90 $\pm$ 0.22	<b>0.87 <math>\pm</math> 0.08</b>
Reddit	GCN	6.69 $\pm$ 0.12	1.64 $\pm$ 0.05	1.64 $\pm$ 0.05	1.45 $\pm$ 0.08	oom	2.20 $\pm$ 0.36	<b>1.02 <math>\pm</math> 0.06</b>
	GAT	4.79 $\pm$ 0.16	3.29 $\pm$ 0.08	3.35 $\pm$ 0.12	0.73 $\pm$ 0.08	oom	1.10 $\pm$ 0.11	<b>0.69 <math>\pm</math> 0.13</b>

## 4.2 Evaluation and Analysis

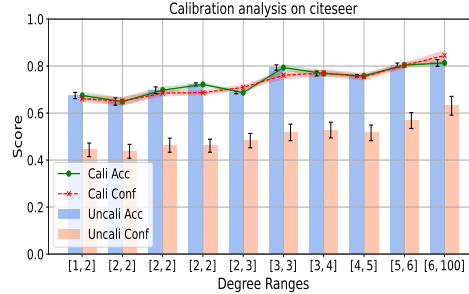
We evaluate the calibration effectiveness of WATS across seven benchmark datasets and two representative GNN architectures (GCN and GAT), with results summarized in Table 1. Empirical findings demonstrate that WATS consistently achieves the lowest ECE in most of scenarios, highlighting its efficacy in leveraging localized, flexibly scaled structural information for post-hoc uncertainty calibration. Beyond achieving superior average ECE scores, WATS also exhibits reduced standard deviations across runs, indicating improved robustness and stability compared to existing methods. These evidence prove that graph wavelet is able to capture sufficient local topology information to correct the confidence level. Moreover, even when the base model is already reasonably well calibrated, for example, on the Photo and Computers, WATS consistently delivers further reductions in calibration error, demonstrating its ability to adaptively refine predictive confidence across a range of baseline reliability levels.

To further illustrate this effect, we visualizes the calibration performance of WATS for Citeseer. The results in Figure 2 shows a comprehensive analysis of calibration performance on the Citeseer dataset. In Figure 2a, the reliability diagram reveals that the uncalibrated model exhibits systematic underconfidence, with predicted probabilities consistently lower actual accuracy across bins. After calibration, the reliability curve aligns more closely with the diagonal, indicating a significant improvement in terms of confidence-accuracy alignment. Figure 2b complements this view by presenting a degree-binned analysis, with the degree increase we can observe a lower uncalibrated ECE, which also compile with our motivation. The uncalibrated model shows a clear mismatch between confidence and accuracy, especially for low-degree nodes, which tend to be the most under-confident. After applying calibration, confidence becomes well-aligned with accuracy across all degree ranges, with reduced standard deviation. This demonstrates that the method effectively improves overall calibration and enhances robustness, particularly for structurally sparse or uncertain regions. Full visualizations about the main experiment are provided in the Appendix.

Furthermore, GATS’s reliance on full attention over a node’s neighborhood leads to poor memory scalability and resulting in out-of-memory failures on large graphs such as Reddit. In contrast, WATS remains efficient by using spectral approximations to compute graph wavelet features, which improve the scalability of WATS.



(a) Reliability diagram on citeseer.



(b) Degree-binned calibration analysis on citeseer.

Figure 2: In both plots, “Uncali” refers to the uncalibrated model and “Cali” refers to the calibrated model. (a) shows the reliability diagram comparing calibrated and uncalibrated outputs. The diagonal dashed line indicates perfect calibration (b) presents a degree-binned analysis of accuracy and confidence. Solid and dashed lines represent calibrated accuracy and confidence respectively. Results are averaged over 10 runs, with error bars indicating standard deviation.

### 4.3 Ablation study

#### 4.3.1 Different graph features

To assess the effectiveness of graph wavelet features in post-hoc calibration, we conduct a comparative analysis against several widely used structural descriptors, including log-degree, betweenness centrality, clustering coefficient, and their various combinations, all evaluated under a consistent GCN-based framework. As summarized in Table 2, wavelet-based representations consistently yield superior calibration performance across most datasets. While certain individual features or their combinations may perform competitively on specific datasets, they tend to exhibit limited generalizability and often result in higher calibration error overall. This highlights the insufficiency of isolated structural indicators and underscores the necessity of incorporating rich, multiscale topological signals. In contrast, graph wavelet features demonstrate both effectiveness and robustness across diverse graph structures, suggesting that the information they encode captures nuanced patterns that cannot be fully replicated by aggregating conventional structural features.

Table 2: Ablation study: ECE ( $\downarrow$ ) comparison between graph wavelet and alternative structural features, where "Deg" denote log transformed degree, "Cen" denote betweenness centrality, "Clus" denote clustering coefficient, and 'oom' indicates out-of-memory failures where the method could not complete. Graph wavelet consistently outperforms other variants across most datasets.

Dataset	Graph wavelet	Deg	Cen	Clus	Deg, Cen	Cen, Clus	Deg, Clus	Deg, Clus, Cen
Citeseer	<b>2.15 ± 0.48</b>	3.53 ± 1.16	3.10 ± 1.05	6.75 ± 1.44	7.24 ± 1.80	7.11 ± 1.80	7.10 ± 1.80	7.12 ± 1.69
Computers	<b>1.31 ± 0.29</b>	1.61 ± 0.33	3.51 ± 0.83	2.75 ± 0.82	1.82 ± 0.22	2.78 ± 0.69	2.60 ± 0.71	2.72 ± 0.66
Cora	2.13 ± 0.51	2.42 ± 0.72	<b>1.86 ± 0.32</b>	4.77 ± 0.40	4.43 ± 0.63	4.51 ± 0.48	4.51 ± 0.48	4.55 ± 0.40
Cora-full	<b>2.04 ± 0.13</b>	3.08 ± 1.34	5.32 ± 0.18	5.66 ± 0.35	5.16 ± 0.23	5.19 ± 0.26	5.19 ± 0.26	5.18 ± 0.25
Photo	<b>1.03 ± 0.18</b>	1.32 ± 0.29	2.23 ± 0.40	1.85 ± 0.38	1.96 ± 0.30	1.93 ± 0.36	1.87 ± 0.34	1.89 ± 0.35
Pubmed	<b>1.04 ± 0.07</b>	1.40 ± 0.35	2.90 ± 0.38	2.30 ± 0.29	1.83 ± 0.20	1.92 ± 0.22	1.93 ± 0.22	1.94 ± 0.20
Reddit	<b>1.02 ± 0.06</b>	1.58 ± 0.17	oom	oom	oom	oom	oom	oom

#### 4.3.2 Sensitivity analysis of graph wavelet hyper-parameters.

To assess the robustness of WATS, we perform an exhaustive grid search over the Chebyshev order  $k \in \{2, 3, 4, 5\}$  and the heat-kernel scale  $s \in \{0.1, 0.4, 0.8, 1.2, 1.6, 2.0, 2.5\}$  on seven node-classification benchmarks, we visualize the changes of ECE for varying  $k$  and  $s$  for Citeseer, Cora, Computers and Reddit on Figure 3 (full results about hyperparameters are in Appendix).

The results demonstrate that calibration quality in heat-kernel graph wavelets is highly sensitive to both the Chebyshev order  $k$  and the diffusion scale  $s$ . Across all evaluated benchmarks, the minimum ECE is consistently obtained when  $k \in \{3, 4\}$ . Orders below this range restrict the receptive field to an overly local neighbourhood, omitting salient meso-scale structure, whereas excessively large orders indiscriminately propagate information from noisy nodes, thereby deteriorating calibration.

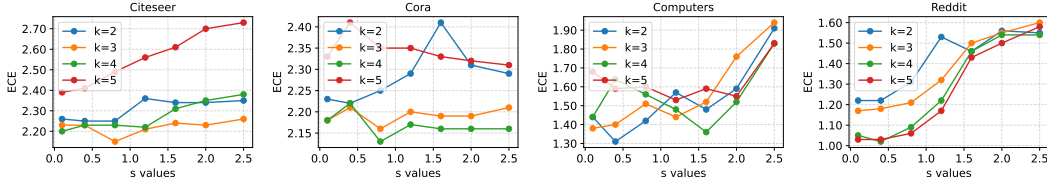


Figure 3: Sensitivity analysis of wavelet scale hyper-parameters. Each plot shows the ECE scores on different datasets with varying wavelet scale parameter  $s$  (x-axis) and polynomial order  $k$ . Each line represents a different Chebyshev order  $k$ : blue for  $k = 2$ , orange for  $k = 3$ , green for  $k = 4$ , and red for  $k = 5$ .

We also observe that lower-connectivity graphs are generally more sensitive to  $k$ , as higher orders tend to introduce additional noise into the calibration process.

The diffusion scale  $s$  exhibits a pronounced dependence on graph connectivity. In densely connected graphs, calibration is markedly sensitive to the choice of  $s$ ; once  $s$  surpasses its dataset-specific optimum, the ECE rises rapidly, indicating severe over-smoothing. By contrast, in sparser graphs, calibration performance is comparatively robust: deviations from the optimal  $s$  induce only gradual changes in ECE, reflecting a more stable trade-off between local and global diffusion.

Importantly, although the result is highly correlated to hyperparameter choices, it remains consistently effective within a broad and practical range, specifically when  $k \in \{3, 4\}$  and  $s \in [0.4, 1.2]$ . Even without fine-tuning, WATS typically outperforms existing calibration methods across this range, confirming its robustness and the strength of wavelet-based structural signals. These findings reinforce the hypothesis that effective calibration is primarily governed by localized structural cues, with densely connected graphs requiring more precise diffusion control.

#### 4.4 Complexity Analysis

We further compare the complexity with other post-hoc calibration method to prove the computational efficiency. Our method consists of two main components: graph wavelet feature extraction and a two-layer MLP for temperature prediction. Let  $k$  be the Chebyshev polynomial order. Each Chebyshev term requires a sparse matrix multiplication, leading to a total time complexity of  $\mathcal{O}(k|\mathcal{E}| + |\mathcal{V}|k)$ , where  $|\mathcal{E}|$  and  $|\mathcal{V}|$  denote the number of edges and nodes, respectively. The first term accounts for  $k$  sparse multiplications over the Laplacian, while the second accounts for the intermediate tensor concatenation and normalization steps. The wavelet features of each node (dimension  $k + 1$ ) are passed through a two-layer MLP with hidden size  $h$ . The per-node computation costs  $\mathcal{O}((k + 1)h)$ , and thus the total cost over all nodes is:  $\mathcal{O}(|\mathcal{V}|kh)$ . Combining the above, the overall time complexity of our method is:

$$\mathcal{O}(k|\mathcal{E}| + |\mathcal{V}|k + |\mathcal{V}|kh) = \mathcal{O}(k|\mathcal{E}| + |\mathcal{V}|kh).$$

Compared to CaGCN [41] with  $\mathcal{O}(|\mathcal{E}|F + |\mathcal{V}|F^2)$ , and GATS [39] with  $\mathcal{O}(|\mathcal{E}|FH + |\mathcal{V}|F^2)$ , our model is significantly more efficient, especially when  $F$  is large or multi-head attention is used. GETS [53] incurs higher cost due to expert selection, with complexity  $\mathcal{O}(k(|\mathcal{E}|F + |\mathcal{V}|F^2) + |\mathcal{V}|MF)$ , where  $k \ll M$ . In practice, the wavelet transformation can be precomputed and reused as a static input.

## 5 Conclusion

We introduce Wavelet-Aware Temperature Scaling (WATS), a lightweight post-hoc calibration framework that assigns node-specific temperature values based on graph wavelet features. By exploiting localized structural representations, WATS effectively captures diverse structural characteristics and implicitly broadens each node’s structural receptive field, thereby enhancing post-hoc information utilization with minimal computational overhead. Experimental results on seven benchmark datasets and two GNN backbones consistently show that WATS achieves the lowest ECE and markedly improves calibration stability, contributing to more reliable and trustworthy GNN predictions, especially for the high risk domains. While if the node distribution is extremely skewed, WATS may tend to be slightly overconfident for the large degree nodes, especially for the sparse graph due to the insufficient samples for calibration training.

Although WATS primarily captures rich topological information, future work could explore integrating structurally similar yet distant neighborhoods to introduce global structural context, which means capture the node with similar structural embedding. This could further enhance calibration performance and robustness, provided that the inclusion of such global information avoids introducing extraneous noise.

## References

- [1] Maysam Behmanesh, Peyman Adibi, Sayyed Mohammad Saeed Ehsani, and Jocelyn Chaussoot. Geometric multimodal deep learning with multiscaled graph wavelet convolutional network. *IEEE Transactions on Neural Networks and Learning Systems*, 2022.
- [2] Aleksandar Bojchevski and Stephan Günnemann. Deep gaussian embedding of graphs: Unsupervised inductive learning via ranking. *arXiv preprint arXiv:1707.03815*, 2017.
- [3] A. Bruce, D. Donoho, and H.-Y. Gao. Wavelet analysis [for signal processing]. *IEEE Spectrum*, 33(10):26–35, 1996. doi: 10.1109/6.540087.
- [4] Mark Crovella and Eric Kolaczyk. Graph wavelets for spatial traffic analysis. In *IEEE INFOCOM 2003. Twenty-second Annual Joint Conference of the IEEE Computer and Communications Societies (IEEE Cat. No. 03CH37428)*, volume 3, pages 1848–1857. IEEE, 2003.
- [5] K Ch Das. The laplacian spectrum of a graph. *Computers & Mathematics with Applications*, 48(5-6):715–724, 2004.
- [6] Swakshar Deb, Sejuti Rahman, and Shafin Rahman. Sea-gwnn: Simple and effective adaptive graph wavelet neural network. *Proceedings of the AAAI Conference on Artificial Intelligence*, 38(10):11740–11748, Mar. 2024. doi: 10.1609/aaai.v38i10.29058. URL <https://ojs.aaai.org/index.php/AAAI/article/view/29058>.
- [7] Claire Donnat, Marinka Zitnik, David Hallac, and Jure Leskovec. Learning structural node embeddings via diffusion wavelets. In *Proceedings of the 24th ACM SIGKDD international conference on knowledge discovery & data mining*, pages 1320–1329, 2018.
- [8] Wenqi Fan, Yao Ma, Qing Li, Yuan He, Eric Zhao, Jiliang Tang, and Dawei Yin. Graph neural networks for social recommendation, 2019. URL <https://arxiv.org/abs/1902.07243>.
- [9] Yarin Gal and Zoubin Ghahramani. Dropout as a bayesian approximation: Representing model uncertainty in deep learning. In *international conference on machine learning*, pages 1050–1059. PMLR, 2016.
- [10] Chao Gao, Shu Yin, Haiqiang Wang, Zhen Wang, Zhanwei Du, and Xuelong Li. Medical-knowledge-based graph neural network for medication combination prediction. *IEEE Transactions on Neural Networks and Learning Systems*, 35(10):13246–13257, 2024. doi: 10.1109/TNNLS.2023.3266490.
- [11] C Lee Giles, Kurt D Bollacker, and Steve Lawrence. Citeseer: An automatic citation indexing system. In *Proceedings of the third ACM conference on Digital libraries*, pages 89–98, 1998.
- [12] Jonathan Godwin, Michael Schaarschmidt, Alexander L. Gaunt, Alvaro Sanchez-Gonzalez, Yulia Rubanova, Petar Velickovic, James Kirkpatrick, and Peter W. Battaglia. Very deep graph neural networks via noise regularisation. *CoRR*, abs/2106.07971, 2021. URL <https://arxiv.org/abs/2106.07971>.
- [13] Chuan Guo, Geoff Pleiss, Yu Sun, and Kilian Q. Weinberger. On calibration of modern neural networks. *CoRR*, abs/1706.04599, 2017. URL <http://arxiv.org/abs/1706.04599>.
- [14] Will Hamilton, Zhitao Ying, and Jure Leskovec. Inductive representation learning on large graphs. *Advances in neural information processing systems*, 30, 2017.
- [15] David K Hammond, Pierre Vandergheynst, and Rémi Gribonval. Wavelets on graphs via spectral graph theory. *Applied and Computational Harmonic Analysis*, 30(2):129–150, 2011.
- [16] Hans Hao-Hsun Hsu, Yuesong Shen, Christian Tomani, and Daniel Cremers. What makes graph neural networks miscalibrated? *Advances in Neural Information Processing Systems*, 35: 13775–13786, 2022.
- [17] Thomas N Kipf and Max Welling. Semi-supervised classification with graph convolutional networks. *arXiv preprint arXiv:1609.02907*, 2016.

- [18] Meelis Kull, Telmo Silva Filho, and Peter Flach. Beta calibration: a well-founded and easily implemented improvement on logistic calibration for binary classifiers. In *Artificial intelligence and statistics*, pages 623–631. PMLR, 2017.
- [19] Tong Liu, Yushan Liu, Marcel Hildebrandt, Mitchell Joblin, Hang Li, and Volker Tresp. On calibration of graph neural networks for node classification. In *2022 International Joint Conference on Neural Networks (IJCNN)*, pages 1–8. IEEE, 2022.
- [20] Haohui Lu and Shahadat Uddin. A weighted patient network-based framework for predicting chronic diseases using graph neural networks. *Scientific reports*, 11(1):22607, 2021.
- [21] Zihan Luo, Hong Huang, Jianxun Lian, Xiran Song, Xing Xie, and Hai Jin. Cross-links matter for link prediction: Rethinking the debiased gnn from a data perspective. In A. Oh, T. Naumann, A. Globerson, K. Saenko, M. Hardt, and S. Levine, editors, *Advances in Neural Information Processing Systems*, volume 36, pages 79594–79612. Curran Associates, Inc., 2023. URL [https://proceedings.neurips.cc/paper\\_files/paper/2023/file/fba4a59c7a569fce120eea9aa9227052-Paper-Conference.pdf](https://proceedings.neurips.cc/paper_files/paper/2023/file/fba4a59c7a569fce120eea9aa9227052-Paper-Conference.pdf).
- [22] David J.C MacKay. Bayesian neural networks and density networks. *Nuclear Instruments and Methods in Physics Research Section A: Accelerators, Spectrometers, Detectors and Associated Equipment*, 354(1):73–80, 1995. ISSN 0168-9002. doi: [https://doi.org/10.1016/0168-9002\(94\)00931-7](https://doi.org/10.1016/0168-9002(94)00931-7). URL <https://www.sciencedirect.com/science/article/pii/0168900294009317>. Proceedings of the Third Workshop on Neutron Scattering Data Analysis.
- [23] Andrew Kachites McCallum, Kamal Nigam, Jason Rennie, and Kristie Seymore. Automating the construction of internet portals with machine learning. *Information Retrieval*, 3:127–163, 2000.
- [24] Gledson Melotti, Cristiano Premebida, Jordan J. Bird, Diego R. Faria, and Nuno Gonçalves. Reducing overconfidence predictions in autonomous driving perception. *IEEE Access*, 10: 54805–54821, 2022. doi: 10.1109/ACCESS.2022.3175195.
- [25] Howard L. Resnikoff and Raymond O. Wells. Wavelet analysis and the geometry of euclidean domains. *Journal of Geometry and Physics*, 8(1):273–282, 1992. ISSN 0393-0440. doi: [https://doi.org/10.1016/0393-0440\(92\)90052-3](https://doi.org/10.1016/0393-0440(92)90052-3). URL <https://www.sciencedirect.com/science/article/pii/0393044092900523>.
- [26] Yaniv Romano, Evan Patterson, and Emmanuel Candes. Conformalized quantile regression. *Advances in neural information processing systems*, 32, 2019.
- [27] Prithviraj Sen, Galileo Namata, Mustafa Bilgic, Lise Getoor, Brian Galligher, and Tina Eliassi-Rad. Collective classification in network data. *AI magazine*, 29(3):93–93, 2008.
- [28] Amit Sharma, Ashutosh Sharma, Polina Nikashina, Vadim Gavrilenko, Alexey Tselykh, Alexander Bozhenyuk, Mehedi Masud, and Hossam Meshref. A graph neural network (gnn)-based approach for real-time estimation of traffic speed in sustainable smart cities. *Sustainability*, 15(15), 2023. ISSN 2071-1050. doi: 10.3390/su151511893. URL <https://www.mdpi.com/2071-1050/15/15/11893>.
- [29] Oleksandr Shchur, Maximilian Mumme, Aleksandar Bojchevski, and Stephan Günnemann. Pitfalls of graph neural network evaluation. *Relational Representation Learning Workshop, NeurIPS 2018*, 2018.
- [30] Weili Shi, Xueying Yang, Xujiang Zhao, Haifeng Chen, Zhiqiang Tao, and Sheng Li. Calibrate graph neural networks under out-of-distribution nodes via deep q-learning. In *Proceedings of the 32nd ACM International Conference on Information and Knowledge Management*, pages 2270–2279, 2023.
- [31] David I Shuman, Sunil K Narang, Pascal Frossard, Antonio Ortega, and Pierre Vandergheynst. The emerging field of signal processing on graphs: Extending high-dimensional data analysis to networks and other irregular domains. *IEEE signal processing magazine*, 30(3):83–98, 2013.

- [32] Jost Tobias Springenberg, Aaron Klein, Stefan Falkner, and Frank Hutter. Bayesian optimization with robust bayesian neural networks. *Advances in neural information processing systems*, 29, 2016.
- [33] Zeyu Sun, Wenjie Zhang, Lili Mou, Qihao Zhu, Yingfei Xiong, and Lu Zhang. Generalized equivariance and preferential labeling for gnn node classification. *Proceedings of the AAAI Conference on Artificial Intelligence*, 36(8):8395–8403, Jun. 2022. doi: 10.1609/aaai.v36i8.20815. URL <https://ojs.aaai.org/index.php/AAAI/article/view/20815>.
- [34] Wim Sweldens. The lifting scheme: A construction of second generation wavelets. *SIAM journal on mathematical analysis*, 29(2):511–546, 1998.
- [35] Boshi Tang, Zhiyong Wu, Xixin Wu, Qiaochu Huang, Jun Chen, Shun Lei, and Helen Meng. Simcalib: Graph neural network calibration based on similarity between nodes. In *Proceedings of the AAAI Conference on Artificial Intelligence*, volume 38, pages 15267–15275, 2024.
- [36] Linwei Tao, Minjing Dong, and Chang Xu. Feature clipping for uncertainty calibration. *Proceedings of the AAAI Conference on Artificial Intelligence*, 39(19):20841–20849, Apr. 2025. doi: 10.1609/aaai.v39i19.34297. URL <https://ojs.aaai.org/index.php/AAAI/article/view/34297>.
- [37] Ryan J Tibshirani, Rina Foygel Barber, Emmanuel Candes, and Aaditya Ramdas. Conformal prediction under covariate shift. *Advances in neural information processing systems*, 32, 2019.
- [38] Nicolas Tremblay and Pierre Borgnat. Graph wavelets for multiscale community mining. *IEEE Transactions on Signal Processing*, 62(20):5227–5239, 2014.
- [39] Petar Veličković, Guillem Cucurull, Arantxa Casanova, Adriana Romero, Pietro Lio, and Yoshua Bengio. Graph attention networks. *arXiv preprint arXiv:1710.10903*, 2017.
- [40] Min Wang, Hao Yang, and Qing Cheng. Gcl: Graph calibration loss for trustworthy graph neural network. In *Proceedings of the 30th ACM International Conference on Multimedia*, pages 988–996, 2022.
- [41] Xiao Wang, Hongrui Liu, Chuan Shi, and Cheng Yang. Be confident! towards trustworthy graph neural networks via confidence calibration. *Advances in Neural Information Processing Systems*, 34:23768–23779, 2021.
- [42] Bingbing Wen, Chenjun Xu, Robert Wolfe, Lucy Lu Wang, Bill Howe, et al. Mitigating overconfidence in large language models: A behavioral lens on confidence estimation and calibration. In *NeurIPS 2024 Workshop on Behavioral Machine Learning*, 2024.
- [43] Bingbing Xu, Huawei Shen, Qi Cao, Yunqi Qiu, and Xueqi Cheng. Graph wavelet neural network. *arXiv preprint arXiv:1904.07785*, 2019.
- [44] Cheng Yang, Chengdong Yang, Chuan Shi, Yawen Li, Zhiqiang Zhang, and Jun Zhou. Calibrating graph neural networks from a data-centric perspective. In *Proceedings of the ACM Web Conference 2024*, pages 745–755, 2024.
- [45] Hao Yang, Min Wang, Qi Wang, Mingrui Lao, and Yun Zhou. Balanced confidence calibration for graph neural networks. In *Proceedings of the 30th ACM SIGKDD Conference on Knowledge Discovery and Data Mining*, pages 3747–3757, 2024.
- [46] Bianca Zadrozny and Charles Elkan. Learning and making decisions when costs and probabilities are both unknown. In *Proceedings of the seventh ACM SIGKDD international conference on Knowledge discovery and data mining*, pages 204–213, 2001.
- [47] Bianca Zadrozny and Charles Elkan. Transforming classifier scores into accurate multiclass probability estimates. In *Proceedings of the eighth ACM SIGKDD international conference on Knowledge discovery and data mining*, pages 694–699, 2002.
- [48] Jize Zhang, Bhavya Kailkhura, and T Yong-Jin Han. Mix-n-match: Ensemble and compositional methods for uncertainty calibration in deep learning. In *International conference on machine learning*, pages 11117–11128. PMLR, 2020.

- [49] Muhan Zhang and Yixin Chen. Link prediction based on graph neural networks. In S. Bengio, H. Wallach, H. Larochelle, K. Grauman, N. Cesa-Bianchi, and R. Garnett, editors, *Advances in Neural Information Processing Systems*, volume 31. Curran Associates, Inc., 2018. URL [https://proceedings.neurips.cc/paper\\_files/paper/2018/file/53f0d7c537d99b3824f0f99d62ea2428-Paper.pdf](https://proceedings.neurips.cc/paper_files/paper/2018/file/53f0d7c537d99b3824f0f99d62ea2428-Paper.pdf).
- [50] Zaixi Zhang, Qi Liu, Hao Wang, Chengqiang Lu, and Chee-Kong Lee. Motif-based graph self-supervised learning for molecular property prediction. In M. Ranzato, A. Beygelzimer, Y. Dauphin, P.S. Liang, and J. Wortman Vaughan, editors, *Advances in Neural Information Processing Systems*, volume 34, pages 15870–15882. Curran Associates, Inc., 2021. URL [https://proceedings.neurips.cc/paper\\_files/paper/2021/file/85267d349a5e647ff0a9edcb5ffd1e02-Paper.pdf](https://proceedings.neurips.cc/paper_files/paper/2021/file/85267d349a5e647ff0a9edcb5ffd1e02-Paper.pdf).
- [51] Tianxiang Zhao, Xiang Zhang, and Suhang Wang. Graphsmote: Imbalanced node classification on graphs with graph neural networks. In *Proceedings of the 14th ACM International Conference on Web Search and Data Mining, WSDM '21*, page 833–841, New York, NY, USA, 2021. Association for Computing Machinery. ISBN 9781450382977. doi: 10.1145/3437963.3441720. URL <https://doi.org/10.1145/3437963.3441720>.
- [52] Xuebin Zheng, Bingxin Zhou, Junbin Gao, Yu Guang Wang, Pietro Lió, Ming Li, and Guido Montúfar. How framelets enhance graph neural networks. *arXiv preprint arXiv:2102.06986*, 2021.
- [53] Dingyi Zhuang, Chonghe Jiang, Yunhan Zheng, Shenhao Wang, and Jinhua Zhao. Gets: Ensemble temperature scaling for calibration in graph neural networks. *arXiv preprint arXiv:2410.09570*, 2024.

## A Experiment setting

We randomly conduct the train test split 10 times for each dataset with identical random seed. We employed the GATS, GETS and CaGCN based on their paper and code. The hyperparameters for backbone GNNs training are based on the complexity of graph data. The detail is given below Table 3.

Table 3: Summary of training parameters of GCN and GAT

Dataset	Hidden Dim.	Dropout	Epochs	Learning Rate	Weight Decay
Citeseer	16	0.5	200	$1 \times 10^{-2}$	$5 \times 10^{-4}$
Computers	64	0.8	200	$1 \times 10^{-2}$	$1 \times 10^{-3}$
Cora-full	64	0.8	200	$1 \times 10^{-2}$	$1 \times 10^{-3}$
Cora	16	0.5	200	$1 \times 10^{-2}$	$5 \times 10^{-4}$
Photo	64	0.8	200	$1 \times 10^{-2}$	$1 \times 10^{-3}$
Pubmed	16	0.5	200	$1 \times 10^{-2}$	$5 \times 10^{-4}$
Reddit	16	0.5	200	$1 \times 10^{-2}$	$5 \times 10^{-4}$

Full details of WATS in calibration is given be on Table 4. Hidden dimension and drop out are chosen based on the data complexity. The hyperparameter of graph wavelet  $k$  and  $s$  are chosen based on the Ablation study.

Table 4: Calibration settings for WATS

Dataset	Hidden Dim.	Dropout	k	s
Citeseer	32	0.4	3	0.8
Computers	64	0.4	2	0.4
Cora-full	128	0.2	4	1.2
Cora	16	0.95	4	0.8
Photo	32	0.4	4	0.4
Pubmed	32	0.4	4	1.6
Reddit	64	0.4	4	0.4

Full details of the Chosen datasets is given on Table 5. It reports the number of nodes, edges, average node degree, input feature dimensions, and number of classes for each dataset. These datasets cover a diverse range of graph sizes, densities, and classification tasks. This diversity ensures a comprehensive evaluation of the proposed method under varying structural and semantic conditions.

Table 5: Summary of selected datasets

Dataset	#Nodes	#Edges	Avg. Degree	#Features	#Classes
Citeseer	3,327	12,431	7.4	3,703	6
Computers	13,381	491,556	73.4	767	10
Cora	2,708	13,264	9.7	1,433	7
Cora-full	18,800	144,170	15.3	8,710	70
Photo	7,487	238,087	63.6	745	8
Pubmed	19,717	108,365	10.9	500	3
Reddit	232,965	114,848,857	98.5	602	41

**Computational Environment.** All experiments are conducted using the following environment with PyTorch 2.4.0 (Python 3.11, CUDA 12.4.1), Hardware: NVIDIA GTX 4090 GPU with 32 GB RAM on Runpod cloud service (Ubuntu 22.04)

## B Hyperparameter analysis results

Here is the full result for the experiment on hyperparameter analysis. Tables 6 to 9 report the calibration performance measured by ECE of WATS under varying graph wavelet hyperparameters, specifically the Chebyshev order  $k \in \{2, 3, 4, 5\}$  and diffusion scale  $s \in \{0.1, 0.4, 0.8, 1.2, 1.6, 2.0, 2.5\}$ . For each dataset, ECE values are presented across a range of  $s$  values.

Table 6: ECE ( $\downarrow$ ) for  $k = 2$  under varying diffusion scale  $s$ .

Dataset	$s=0.1$	$s=0.4$	$s=0.8$	$s=1.2$	$s=1.6$	$s=2.0$	$s=2.5$
Citeseer	$2.26 \pm 0.68$	$2.25 \pm 0.66$	$2.25 \pm 0.64$	$2.36 \pm 0.72$	$2.34 \pm 0.72$	$2.34 \pm 0.72$	$2.35 \pm 0.74$
Computers	$1.44 \pm 0.26$	$1.31 \pm 0.29$	$1.42 \pm 0.24$	$1.57 \pm 0.35$	$1.48 \pm 0.46$	$1.59 \pm 0.43$	$1.91 \pm 0.64$
Photo	$1.31 \pm 0.31$	$1.29 \pm 0.24$	$1.59 \pm 0.43$	$1.87 \pm 0.34$	$1.99 \pm 0.48$	$2.10 \pm 0.48$	$2.27 \pm 0.45$
Cora	$2.23 \pm 0.70$	$2.22 \pm 0.65$	$2.25 \pm 0.66$	$2.29 \pm 0.67$	$2.41 \pm 0.70$	$2.31 \pm 0.69$	$2.29 \pm 0.72$
Pubmed	$1.13 \pm 0.09$	$1.12 \pm 0.10$	$1.09 \pm 0.10$	$1.10 \pm 0.10$	$1.05 \pm 0.11$	$1.07 \pm 0.13$	$1.20 \pm 0.43$
Cora-full	$2.82 \pm 0.37$	$2.75 \pm 0.36$	$2.76 \pm 0.52$	$2.40 \pm 0.66$	$2.68 \pm 1.40$	$4.93 \pm 1.06$	$5.27 \pm 0.24$
Reddit	$1.22 \pm 0.08$	$1.22 \pm 0.09$	$1.31 \pm 0.19$	$1.53 \pm 0.18$	$1.46 \pm 0.16$	$1.56 \pm 0.10$	$1.55 \pm 0.09$

Table 7: ECE ( $\downarrow$ ) for  $k = 3$  under varying diffusion scale  $s$ .

Dataset	$s=0.1$	$s=0.4$	$s=0.8$	$s=1.2$	$s=1.6$	$s=2.0$	$s=2.5$
Citeseer	$2.23 \pm 0.50$	$2.23 \pm 0.52$	$2.15 \pm 0.48$	$2.21 \pm 0.51$	$2.24 \pm 0.52$	$2.23 \pm 0.50$	$2.26 \pm 0.49$
Computers	$1.38 \pm 0.32$	$1.40 \pm 0.35$	$1.51 \pm 0.20$	$1.44 \pm 0.21$	$1.52 \pm 0.28$	$1.76 \pm 0.54$	$1.94 \pm 0.75$
Photo	$1.07 \pm 0.18$	$1.22 \pm 0.54$	$1.48 \pm 0.58$	$1.63 \pm 0.53$	$2.00 \pm 0.46$	$2.11 \pm 0.48$	$2.22 \pm 0.46$
Cora	$2.18 \pm 0.44$	$2.21 \pm 0.46$	$2.16 \pm 0.46$	$2.20 \pm 0.62$	$2.19 \pm 0.62$	$2.19 \pm 0.62$	$2.21 \pm 0.61$
Pubmed	$1.19 \pm 0.09$	$1.14 \pm 0.09$	$1.13 \pm 0.13$	$1.10 \pm 0.11$	$1.08 \pm 0.10$	$1.18 \pm 0.50$	$1.34 \pm 0.62$
Cora-full	$2.75 \pm 0.21$	$2.82 \pm 0.24$	$2.51 \pm 0.37$	$2.32 \pm 0.53$	$3.24 \pm 1.58$	$4.81 \pm 0.96$	$5.25 \pm 0.29$
Reddit	$1.17 \pm 0.08$	$1.18 \pm 0.07$	$1.21 \pm 0.16$	$1.32 \pm 0.19$	$1.50 \pm 0.15$	$1.55 \pm 0.07$	$1.60 \pm 0.11$

Table 8: ECE ( $\downarrow$ ) for  $k = 4$  under varying diffusion scale  $s$ .

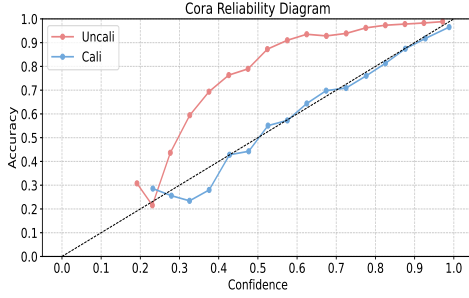
Dataset	$s=0.1$	$s=0.4$	$s=0.8$	$s=1.2$	$s=1.6$	$s=2.0$	$s=2.5$
Citeseer	$2.39 \pm 0.99$	$2.41 \pm 0.62$	$2.49 \pm 1.02$	$2.56 \pm 0.97$	$2.61 \pm 0.94$	$2.70 \pm 0.99$	$2.73 \pm 0.98$
Computers	$1.68 \pm 0.20$	$1.59 \pm 0.27$	$1.60 \pm 0.17$	$1.53 \pm 0.22$	$1.59 \pm 0.43$	$1.55 \pm 0.29$	$1.83 \pm 0.61$
Photo	$1.06 \pm 0.17$	$1.03 \pm 0.18$	$1.39 \pm 0.54$	$1.63 \pm 0.57$	$1.86 \pm 0.43$	$2.03 \pm 0.45$	$2.12 \pm 0.39$
Cora	$2.18 \pm 0.52$	$2.22 \pm 0.52$	$2.13 \pm 0.51$	$2.17 \pm 0.53$	$2.16 \pm 0.52$	$2.16 \pm 0.51$	$2.16 \pm 0.50$
Pubmed	$1.19 \pm 0.10$	$1.22 \pm 0.10$	$1.16 \pm 0.09$	$1.11 \pm 0.08$	$1.04 \pm 0.07$	$1.07 \pm 0.09$	$1.06 \pm 0.08$
Cora-full	$2.53 \pm 0.38$	$2.49 \pm 0.32$	$2.32 \pm 0.24$	$2.04 \pm 0.24$	$3.26 \pm 1.52$	$4.76 \pm 1.07$	$5.19 \pm 0.29$
Reddit	$1.05 \pm 0.06$	$1.02 \pm 0.06$	$1.09 \pm 0.23$	$1.22 \pm 0.21$	$1.46 \pm 0.13$	$1.54 \pm 0.07$	$1.54 \pm 0.08$

Table 9: ECE ( $\downarrow$ ) for  $k = 5$  under varying diffusion scale  $s$ .

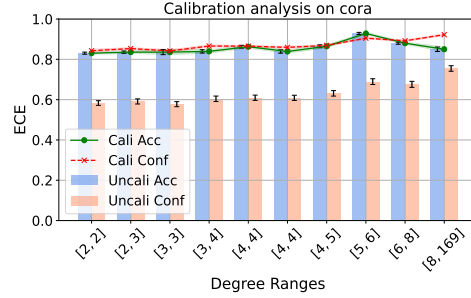
Dataset	$s=0.1$	$s=0.4$	$s=0.8$	$s=1.2$	$s=1.6$	$s=2.0$	$s=2.5$
Citeseer	$2.20 \pm 0.49$	$2.23 \pm 0.49$	$2.23 \pm 0.49$	$2.22 \pm 0.54$	$2.31 \pm 0.46$	$2.35 \pm 0.44$	$2.38 \pm 0.45$
Computers	$1.44 \pm 0.32$	$1.64 \pm 0.24$	$1.56 \pm 0.20$	$1.48 \pm 0.25$	$1.36 \pm 0.27$	$1.52 \pm 0.32$	$1.83 \pm 0.54$
Photo	$1.12 \pm 0.42$	$1.38 \pm 0.68$	$1.52 \pm 0.75$	$1.78 \pm 0.68$	$1.98 \pm 0.51$	$2.09 \pm 0.47$	$2.18 \pm 0.45$
Cora	$2.33 \pm 0.72$	$2.41 \pm 0.74$	$2.35 \pm 0.76$	$2.35 \pm 0.75$	$2.33 \pm 0.75$	$2.32 \pm 0.75$	$2.31 \pm 0.75$
Pubmed	$1.20 \pm 0.11$	$1.23 \pm 0.12$	$1.17 \pm 0.08$	$1.17 \pm 0.11$	$1.13 \pm 0.10$	$1.09 \pm 0.12$	$1.09 \pm 0.12$
Cora-full	$2.65 \pm 0.90$	$2.34 \pm 0.30$	$2.26 \pm 0.23$	$1.90 \pm 0.32$	$2.89 \pm 1.53$	$4.09 \pm 1.58$	$5.16 \pm 0.31$
Reddit	$1.03 \pm 0.07$	$1.03 \pm 0.07$	$1.06 \pm 0.10$	$1.17 \pm 0.15$	$1.43 \pm 0.16$	$1.50 \pm 0.09$	$1.58 \pm 0.11$

## C Full WATS visualizations

We provide the full visualizations of the calibration performance for WATS. Figures 4 to 9 illustrate the calibration performance of WATS on the other datasets. Each figure includes (a) a reliability diagram showing the alignment between predicted confidence and actual accuracy, and (b) a degree-binned analysis comparing confidence and accuracy before and after calibration. Results show that WATS significantly improves calibration and reduces the discrepancy between accuracy and confidence across all degree ranges and all confidence levels. Error bars indicate standard deviation over 10 runs.

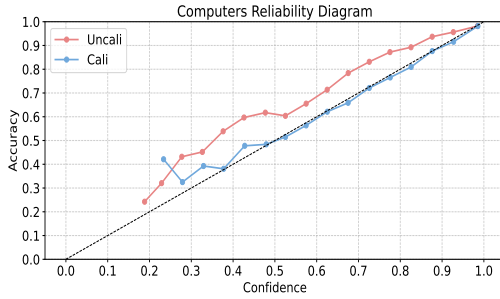


(a) Reliability diagram on Cora.

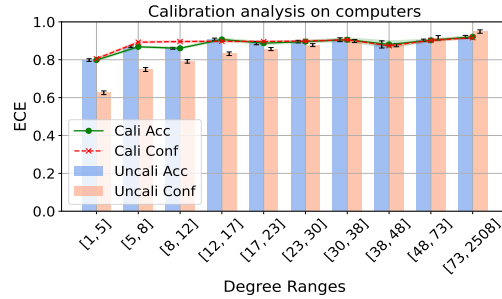


(b) Degree-binned calibration analysis on Cora.

Figure 4: Calibration performance of Cora dataset.

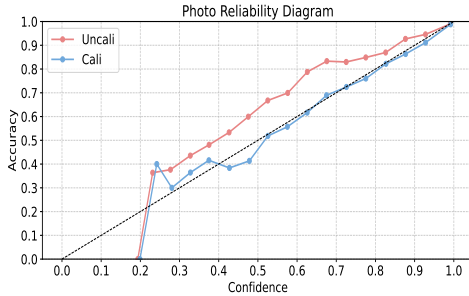


(a) Reliability diagram on Computers.

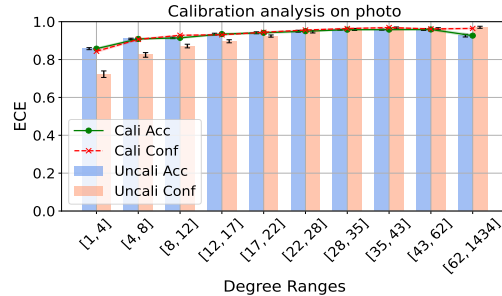


(b) Degree-binned calibration analysis on Computers.

Figure 5: Calibration performance of Computers dataset.

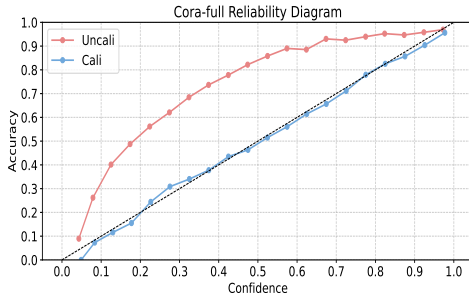


(a) Reliability diagram on Photo.

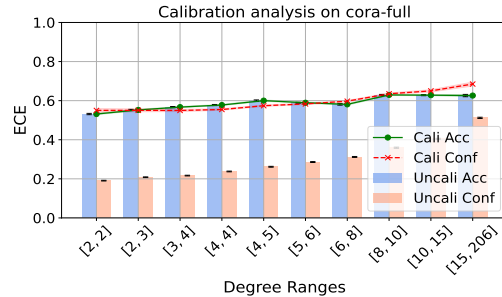


(b) Degree-binned calibration analysis on Photo.

Figure 6: Calibration performance of Photo dataset.

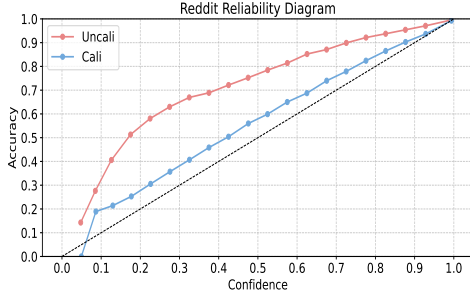


(a) Reliability diagram on Cora-full.

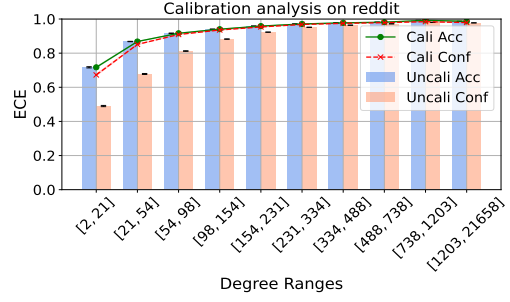


(b) Degree-binned calibration analysis on Cora-full.

Figure 7: Calibration performance of Cora-full dataset.

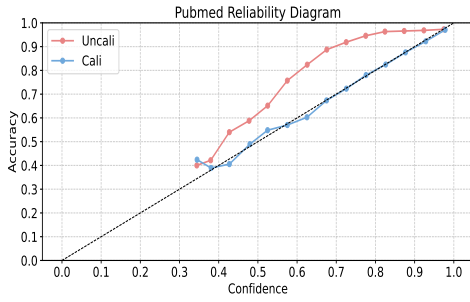


(a) Reliability diagram on Reddit.

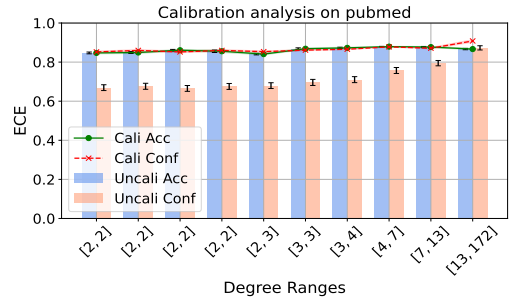


(b) Degree-binned calibration analysis on Reddit.

Figure 8: Calibration performance of Reddit dataset.



(a) Reliability diagram on Pubmed.



(b) Degree-binned calibration analysis on Pubmed.

Figure 9: Calibration performance of Pubmed dataset.